Int j simul model 23 (2024) 4, 575-586
Original scientific paper

EVALUATION OF MEASUREMENT UNCERTAINTY CONTRIBUTIONS IN RING GAUGE CALIBRATION

Acko, B.; Tompa, J. & Klobucar, R.
University of Maribor, Faculty of Mechanical Engineering, Smetanova 17, SI–2000 Maribor, Slovenia
E-Mail: bojan.acko@um.si, jasna.tompa@um.si, rok.klobucar@um.si

Abstract
Measurements are of paramount importance in industry and other areas of importance to society. They are used to determine the characteristics of processes and products, to control and regulate processes, to decide on the acceptable quality of products, etc. To ensure the quality of measurements, we have to calibrate measuring devices regularly. In our laboratory – the holder of the national length standard, we mainly calibrate high-precision standards from accredited laboratories. As the demands on the accuracy of measurements are constantly increasing, we are also forced to continuously improve the accuracy of our calibration procedures. This article presents the development of methods for calibrating the diameter of ring gauges, which represent an important standard for calibrating measuring instruments for measuring internal dimensions. The main objective of this development is to reduce the measurement uncertainty based on a scientific investigation of all influencing parameters. The presented study focuses in particular on the control and reduction of the influence of geometric anomalies of the calibrated rings on the measurement uncertainty during calibration.
(Received in July 2024, accepted in October 2024. This paper was with the authors 1 month for 2 revisions.)

Key Words: Measurement Traceability, Calibration, Measurement Uncertainty, Ring Gauge, Error Simulation

1. INTRODUCTION

In all sectors of the economy, quality control of production and service processes is a key factor for competitiveness on the market. In modern society, the quality of products and services is the most important criterion for evaluating the performance of companies. Adequate and reliable measuring equipment that is properly monitored and maintained is essential for the successful control of production processes. The metrological properties of the measuring equipment are determined by calibration, which must be carried out reliably and with 'traceable' standards [1]. Traceability of a measurement means that the measurement result is related to the definition of the unit of the metrological quantity. The traceability chains usually involve in-house calibration laboratories, accredited laboratories that offer services on the market and national metrology laboratories [2].

In the field of dimensional measurements, industry is constantly faced with demanding challenges in terms of the accuracy and complexity of measurements. Tolerances in the micrometre range for complex products are no longer a rarity [3, 4]. To solve such measurement problems, sophisticated measurement systems are required, including precision sensors with nanometre resolution and coordinate measuring machines that must be regularly calibrated with very precise physical and optical standards (e.g. gauge blocks, ring and plug gauges, step gauges and line scales) [5]. In the Laboratory for Production Measurement of the FS UM, which is responsible for the national length standard, practically all research and development work is focussed on developing new methods and improving the measurement reliability of existing procedures for calibrating physical and optical standards. All procedures are based on the use of laser interferometry and the development of thermally and mechanically stable measuring systems [6]. Current developments are also aimed at improving the method and procedure for calibrating ring gauges, which are an important standard for calibrating instruments for measuring internal dimensions. The aim of this development is a novel absolute calibration

method that enables measurements with significantly reduced uncertainty compared to the calibration procedures currently used in the laboratory. The development work is based, among other things, on scientific analyses of all parameters influencing the measurement result, of which the geometric irregularities of the calibrated rings represent a significant contribution to the measurement uncertainty. The aim of this part of the research is to determine the influence of different types of geometric anomalies by simulating the variations of deviations from the ideal geometric shape of the cylinder. Based on the research results, we will be able to determine the permissible limits of these deviations for certain classes of measurement uncertainties.

2. REVIEW OF EXISTING METHODS AND PROCEDURES FOR CALIBRATING RING DIAMETERS IN THE LABORATORY

2.1 Two-point method and calibration procedure on a universal 1D measuring machine

This is a traditional measuring method that was accredited at the beginning of this century. As standard, we use a Zeiss ULM 600 universal measuring machine (Fig. 1) or a laser interferometer and a set of 50 mm, 150 mm and 250 mm standard rings [5]. The traceability of the measuring machine and the laser interferometer is established by an internal calibration, while the standard rings are calibrated in one of the national European laboratories.

Figure 1: Calibration of the ring diameter on a universal 1D machine by applying laser interferometer as a standard.

The minimum diameter that can be calibrated using this procedure is 12 mm, with an upper limit of 300 mm.

The calibration procedure is as follows:

- First, the two-sensor system is calibrated on a reference ring (setting an initial dimension of 50 mm for rings between 12 mm and 100 mm, 150 mm for rings > 100 mm to 200 mm and 250 mm for rings > 200 mm to 300 mm).
- The ring to be calibrated is then installed and physically aligned. During this alignment, the so-called inflexion point is localised in two directions. The determination of the inflexion point is decisive for the accuracy of the measurement result and therefore one of the main factors for the measurement uncertainty.
- After levelling, the two-point distance is measured in the selected direction and at the selected depth. To determine the effect of the deviation of the ring shape from the ideal shape on the measurement uncertainty, the diameters at five other surrounding points are measured.

The calibration and measurement capability (CMC) of this procedure amounts to:

$$U = \sqrt{(0{,}6\ \mu\text{m})^2 + (3 \cdot 10^{-6} \cdot L)^2}; k = 2 \quad (1)$$

where L is measured length and k is coverage factor for calculating expanded uncertainty.

2.2 Two-point method and calibration procedure on a coordinate measuring machine (CMM)

This method is currently used to calibrate ring gauges in the laboratory. The calibration procedure was accredited about 15 years ago [7]. The CMM used is a Zeiss UMC 850 and a set of 14 mm, 50 mm and 150 mm reference (standard) rings (Fig. 2). The traceability of the measuring machine is established by an internal calibration, while the standard ring gauges have to be calibrated in one of the European national laboratories. The internal calibration of the CMM is carried out according to the comparison principle. A traceable reference ring is measured and the resulting dimension is compared with the calibrated ring gauge diameter. The difference is used as a correction value when calibrating an unknown ring gauge. The measurement uncertainty of the comparator method is assessed using a special procedure.

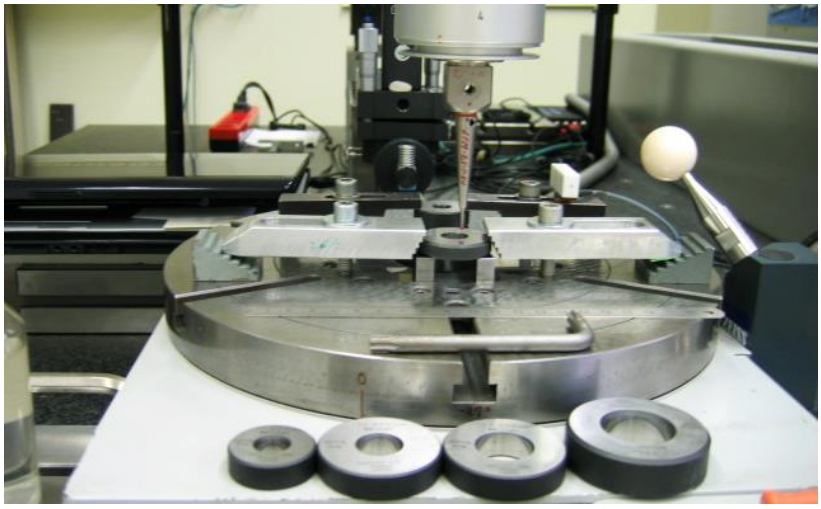

Figure 2: Calibration of a ring gauge by applying a comparator method on a CMM.

The measuring range for this procedure is limited to diameters from 2 mm to 300 mm. It is important that the reference and calibration ring gauges are close to each other and that the temperature difference between the rings is as small as possible. Measurements are always taken in the y-axis, which experience has shown to have the lowest systematic error. Depending on the dimensions of the ring gauge to be measured, the appropriate size of the reference ring and the probe diameter are selected.

The calibration and measurement capability (CMC) of this procedure amounts to:

$$U = \sqrt{(0.2\ \mu\text{m})^2 + (2.8 \times 10^{-6} \times L)^2}; k = 2 \quad (2)$$

for the whole calibration range.

2.3 Scanning method and calibration procedure on a CMM

This method is used to calibrate ring gauges at the special request of customers. These are usually industrial rings where the full circumferential diameter is important. The calibration procedure is practically identical to the two-point procedure presented in section 2.2 and is also accredited. The only difference is the way in which the ring is probed.

The calibration and measurement capability (CMC) is a bit worse than that of the two-point method due to the roundness deviations of the reference rings and is expressed by Eq. (2) for diameters from 2 mm to 120 mm, and by Eq. (3) for diameters from 125 mm to 300 mm:

$$U = \sqrt{(0.6\ \mu\text{m})^2 + (2.8 \times 10^{-6} \times L)^2}; k = 2 \quad (3)$$

2.4 Method and procedure on an integrated system CMM – laser interferometer (LI)

This 2-point method was developed in the laboratory in 2010. In fact, it is a universal method for absolute measurements of internal and external dimensions. Laser interferometer is integrated on the CMM with the purpose of precise linear dimension measurement in y–axis [8]. Special flat mirror interferometer is used for these measurements (Fig. 3). The measurement standard in this procedure is laser interferometer, while a set of gauge blocks and ring gauges are used in addition for determining probe ball diameter.

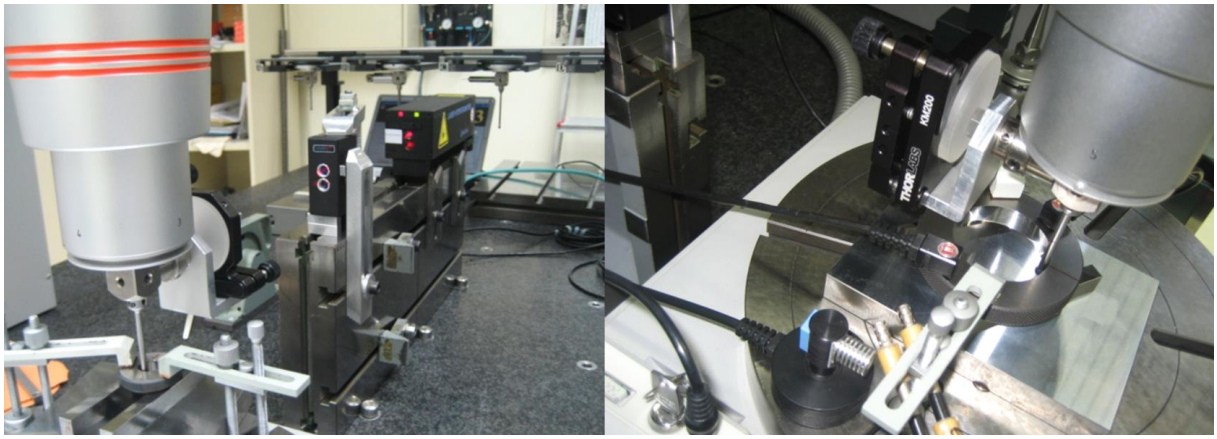

Figure 3: Calibration of a ring gauge on an integrated system CMM – LI.

The calibration and measurement capability (CMC) of this procedure amounts to:

$$U = \sqrt{(0.6\ \mu\text{m})^2 + (2 \times 10^{-6} \times L)^2}; k = 2 \quad (4)$$

for the whole calibration range.

2.5 Method and procedure on a customised measurement system based on a custom-made 2D NC stage

The base for the measurement setup for this calibration procedure is a numerically controlled 2D stage with a resolution in the sub-micrometre range, which was manufactured according to our own design by the company Newport Spectra Physics (Fig. 4). The measurement setup was developed in our laboratory as a universal reference measuring system for the calibration of various physical length standards such as gauge blocks, step gauges, gap gauges, thickness gauges, outer cylinders and ring gauges [9]. It consists of the following components:

- Base – NC-controlled 2D table,
- Laser interferometer setup for linear displacement and angle optics,
- Bi-directional inductive measuring probe,
- Temperature measurement system with 5 material and 2 air thermistor sensors.

The calibration procedure is still in the development phase. It will be fully automatic and allow a large number of measurement repetitions without human intervention in order to reduce random errors to a few nanometres. A LabView application links the acquired data from the stage (coordinates), the laser interferometer (measured lengths) and the temperature measurement system (material and air temperatures to correct for thermal expansion and the refractive index of the air). It will also create an interface between the operator and the measurement setup. A user-friendly operating screen is already under construction. Some experience from other procedures for calibrating step gauges and thickness gauges will be incorporated.

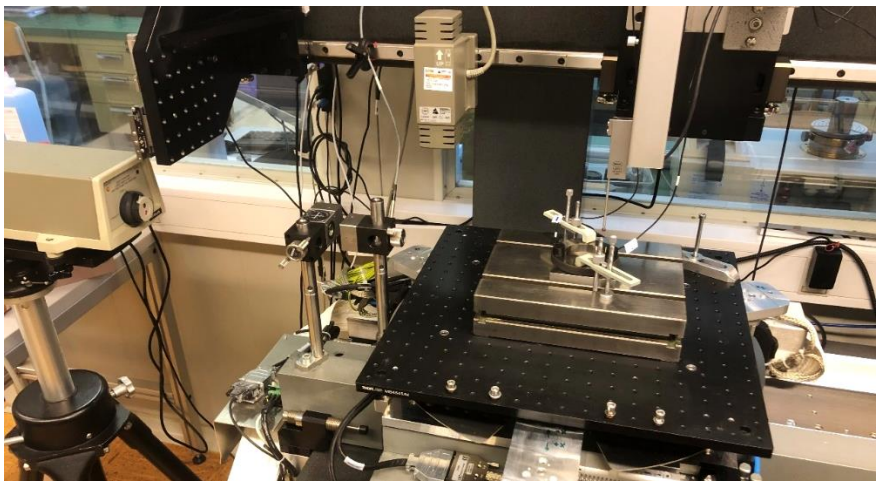

Figure 4: Calibration of a ring gauge on a customised measurement system.

Particular attention will be paid to the adjustment of the ring gauge before calibration. The measurand on a measuring ring is a two–point circle diameter. This circle is an intersection of the cylinder with a plane that is perpendicular to the cylinder axis. It should be noted that the cylinder does not form an ideal perpendicular to either the upper or lower surface (plane) of the ring gauge. Therefore, these boundary surfaces (planes) cannot be used to set the cylinder. The measuring line for determining the two–point diameter must run through the centre of a circle in the selected cylinder section plane and be perpendicular to the cylinder axis. After a preliminary physical ring gauge adjustment, a special algorithm ensures the final alignment of the measured variable to the machine axis. The coordinates of selected pre-tested points on the cylinder are used as input data for the algorithm.

3. MEASUREMENT UNCERTAINTY

3.1 Important contributions

Contributions to the measurement uncertainty are in general random errors and residues of systematic errors. Random errors can be diminished by repeating measurements under unchanged conditions, while the systematic error residuals depend on the quality of evaluating and removing systematic influential quantities.

Main contribution quantities to the measurement uncertainty of described ring gauge calibration procedures are more or less same. Therefore, only the uncertainty budget for the procedure described in 2.5 will be analysed in detail in this chapter. The following systematic error residuals play significant role:

- Laser interferometer (LI) bias depending on the determination and stability of laser light frequency, as well as on determination of refraction index of air based on air temperature, pressure and humidity measurement); calibration uncertainties of the laser frequency and air sensors (T, p, H) are included in this contribution,
- Dead path error depending on the adjustment of the LI optics at the reference point,
- Inductive probe bias determination (calibration uncertainty),
- Probe ball diameter determination (calibration uncertainty),
- Thermal expansion of the ring gauge depending on the ring gauge temperature and the linear thermal expansion coefficient,
- Cosine error (4 components – ring gauge and laser beam adjustment in 2 perpendicular planes),
- Error due to the misalignment of the actual measurement direction in relation to the nominal direction (through the ring gauge centre perpendicularly to the cylinder axis).

While the first five significant contributions have been studied in detail through the existing ring gauge procedure and similar distance calibration procedures, the last one has always been assumed to be negligible. However, since the new calibration procedure under development (section 2.5) includes specific ring gauge and laser beam adjustment, it is important to discover the adjustment influences and to set limitations in relation to the targeted total measurement uncertainty. The uncertainty budget with the limit of the measurement direction adjustment contribution is presented in Table I.

The symbols in Table I represent the following quantities (significant contributions to the measurement uncertainty):

- L_{LI} – compensated length shown by the LI in the measurement point,
- L_T – bi-directional probe indication in the measurement point,
- d_k – sphere diameter of the bi-directional probe,
- L_{ref} – sum of the LI and the bi-directional probe indications in the reference (zero) position (assumed value is 0; reset),
- α_m – linear temperature expansion coefficient of the ring gauge,
- θ_m – temperature deviation of the step gauge from 20 °C,
- e_{tcm} – error of the thermal expansion calculation (compensation formula),
- e_{cos} – cosine error (assumed to be 0),
- e_{ms} – dead path error,
- e_a – error due to the table tilt and rotation (Abbe error),
- e_{ms} – random error due to non-compensated mechanical influences (repeatability),
- l_{ad} – determined limit of the measurement direction adjustment contribution.

Table I: Uncertainty budget of the ring gauge diameter measurement.

Quantity X_i	**Estimated value**	**Standard uncertainty**	**Distribution**	**Sensitivity coefficient**	**Uncertainty contribution**
L_{LI}	L	10 nm + 2 × 10^{-7} × L	normal	1	10 nm + 2 × 10^{-7} × L
L_T	<100 nm	20 nm	normal	1	20 nm
d_k	3 mm	30 nm		1	30 nm
L_{ref}	0 mm	17 nm	normal	-1	17 nm
α_m	11 × 10^{-6} °C^{-1}	0.58 × 10^{-6} °C^{-1}	rectangular	0.1 °C × L	6 × 10^{-8} × L
θ_m	0 °C	0.0075 °C	normal	11 × 10^{-6} °C^{-1} × L	8.3 × 10^{-8} × L
e_{tcm}	0	3 × 10^{-8} × L	rectangular	-1	3 × 10^{-8} × L
e_{cos}	0	1.3 × 10^{-8} × L	rectangular	1	1.3 × 10^{-8} × L
e_{mp}	0	9 nm	rectangular	1	9 nm
e_a	0	13 nm	rectangular	1	14 nm
e_{ms}	0	11 nm	normal	1	11 nm
l_{ad}	50 nm	25 nm	normal	1	25 nm
				Total:	$\sqrt{(52\ \text{nm})^2 + (2.3 \times 10^{-7} \times L)^2}$

The limit l_{ad} was determined in accordance with the targeted maximum measurement uncertainty of the calibration procedure. Adjustment of the ring gauge and simulation of the adjustment error contributions in relation to the geometrical irregularities of the ring is presented in the following paragraph.

4. RING GAUGE ADJUSTMENT AND IT'S CONTRIBUTION TO THE MEASUREMENT UNCERTAINTY

4.1 Basic adjustment principle

Ring gauge adjustment is already briefly described in the last paragraph of section 2.5. The measurement direction shall go through the circle centre in the horizontal measurement plane that is perpendicular to the (vertical) cylinder axis as indicated in Fig. 5. The calibration procedure approach is to set the vertical adjustment line through one line on the cylinder (Fig. 5). This line is representing cylinder axis direction in measurement.

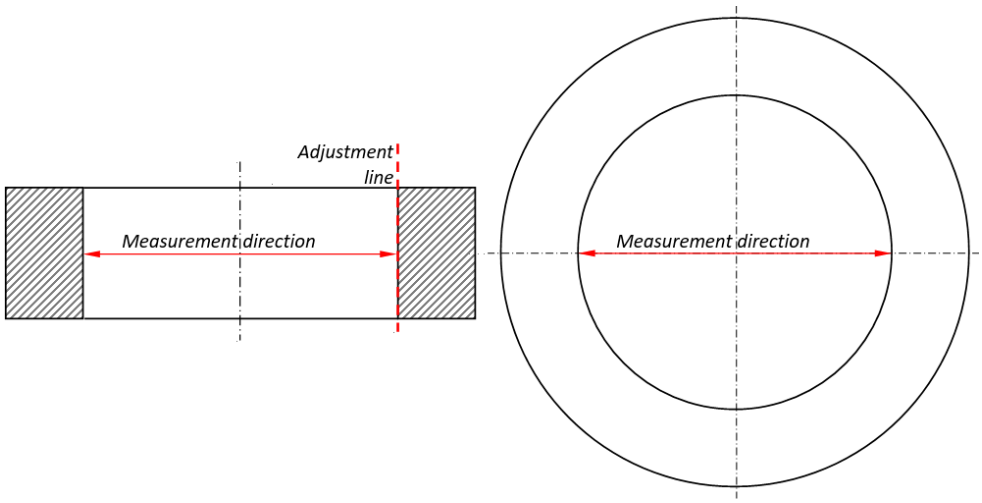

Figure 5: Basic ring gauge adjustment principle.

4.2 Adjustment deviations

Adjustment deviations are influenced by measurement errors and geometrical imperfections of the ring gauge to be calibrated. Fig. 6 is representing adjustment deviation due to the measurement errors on a "perfect" ring without geometrical irregularities.

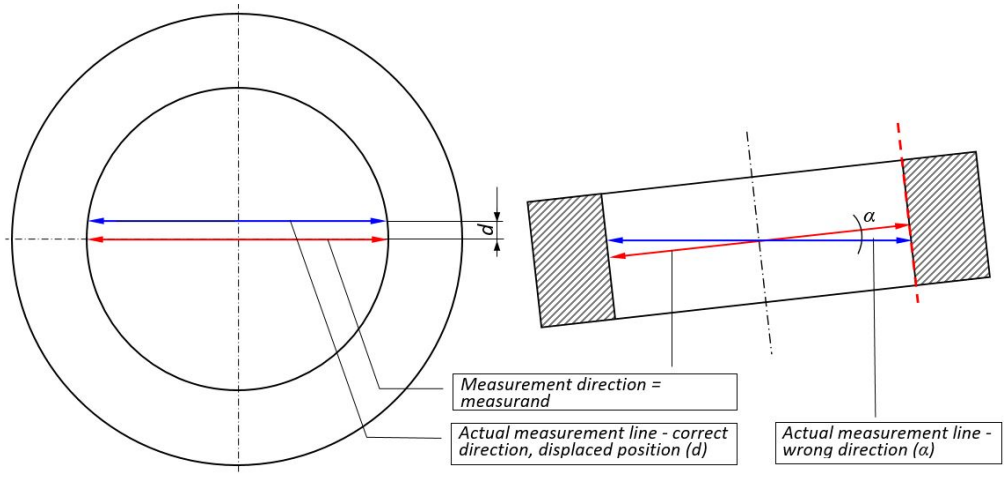

Figure 6: Illustration of displaced measurement lines in relation to the measurand.

The left side of Fig. 6 is illustrating displaced measurement line in horizontal plane (displacement d) due to the positioning error of the measuring device, while the rotation of the measurement direction (α) on the right side is a consequence of probing error on the adjustment line (red dashed line).

While the displacement of the measurement line in horizontal position is not depending on the geometrical irregularities, the adjustment of the cylinder axis position can depend on the cylinder irregularities. Most common cylinder shape deviations like conical, concave and convex, as well as axis perpendicularity deviation are illustrated in Fig. 7.

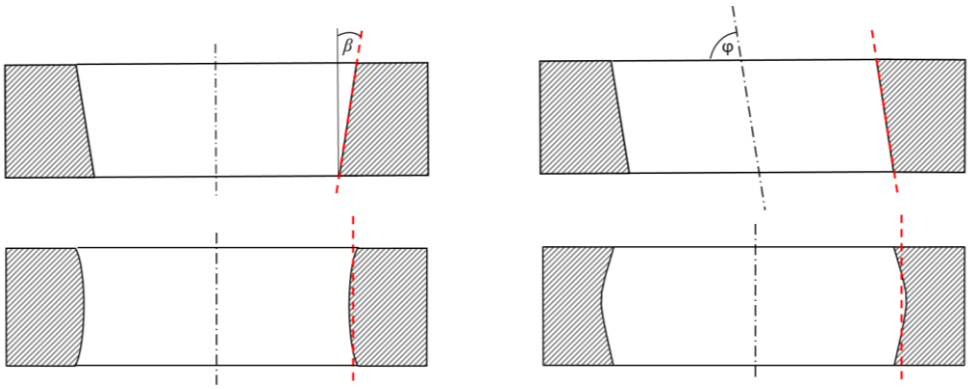

Figure 7: Most common cylinder shape and position deviations.

The major influencing geometrical deviation on the axis direction determination is conical shape, since the adjustment line in our procedure is the red dashed line in Fig. 7.

4.3 Relations between the adjustment deviations and the diameter measurement error

The diameter measurement error caused by the ring gauge misalignment is the difference in lengths between the actual measurement line (blue line in Fig. 6) and the measurand (red line in Fig. 6). This difference can be evaluated quite simply for the ideal cylindrical shape of the ring gauge, while the calculation for irregular shapes such as ellipse and Reuleaux Triangle (or other Reuleaux Polygons) is not so trivial. Therefore, simulations were made in MathLab for these shapes.

The relation between the diameter measurement error (e_d) and the measurement line displacement ("d" in Fig. 6) on a perfect circle with the dimeter D is expressed by Eq. (5), while the relation of the error and the angular direction deviation (α in Fig. 6) is expressed by Eq. (6).

$$e_d = 2\sqrt{(D/2)^2 - d^2} - D \tag{5}$$

$$e_\alpha = D(\,1/cos\alpha - 1) \tag{6}$$

where:

- e_d – measurement error caused by the measurement line displacement,
- e_α – measurement error caused by the measurement line angular direction deviation,
- D – cylinder diameter,
- d – displacement of the measurement line from the nominal measurement direction,
- α – angle between the nominal and actual measurement direction (Fig. 6).

4.4 Simulation of the diameter measurement errors for different deviation cases

Boundary conditions for simulating different cases of the measurement direction misalignment on cylinders with geometrical imperfections were set in accordance with the practical experiences in calibrating setting rings and high precision reference rings in the calibration laboratory. Since the simulation serves for determining laboratory calibration and measurement capability (CMC), only high precision ring gauges were considered. Industrial rings with quite high shape deviations and damages were not subject of this research. Boundary values of the concerned quantities are presented in Table II.

Table II: Experimentally determined boundary values for quantities to be simulated.

Roundness deviation ***R***	**Cone angle** ***β***	**Axis angle to top surface** ***φ***	**Axis displacement** ***d***	**Axis angular misalignment** ***α***
5 µm	0,02°	0,02°	20 µm	0,02°

The maximum roundness deviation was considered in the simulation of the axis displacement d (Fig. 6) on elliptical and triangular (Reuleaux triangle) shapes in different orientations, while the maximum cone angle β and the maximum axis angle to the top of the ring φ (β and φ shown in Fig. 7) were considered in the simulation of the influence of the axis angle displacement α (Fig. 6). The simulation cases are shown in Fig. 8. Red lines in presented cases represent nominal measurement direction (measurand), while the blue line is indicating real measurement direction. The distance between the blue and the red line in Cases 2 to 8 is the displacement error of the real measurement line d (see also Fig. 6), while the angle between the blue and the red line in Case 1 is the axis rotational error caused by imperfect probing of the adjustment line (illustrated in Fig. 5).

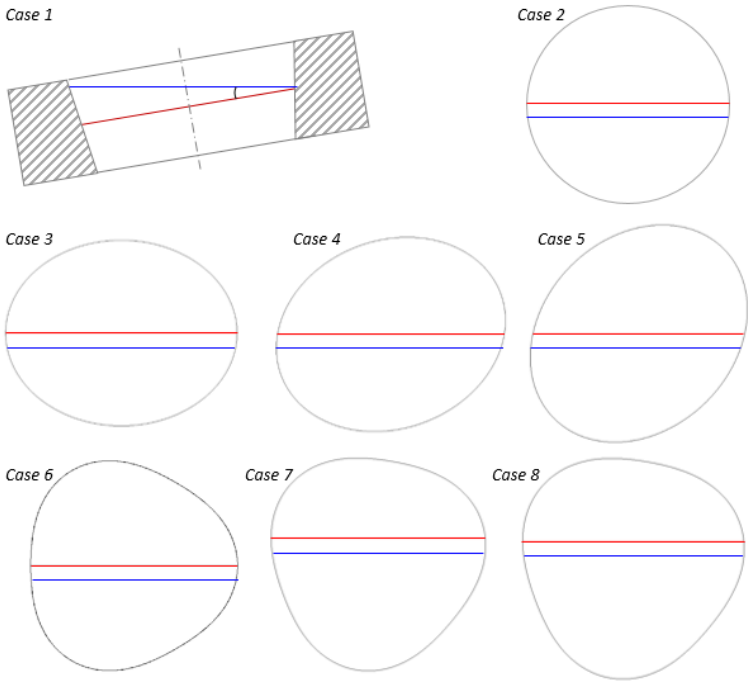

Case 1: Conical shape of the cylinder (rotational error)

Case 2: Displaced measurement line on a perfect circle

Case 3: Displaced measurement line on an elliptical shape (oriented along the measurement axis)

Case 4: Displaced measurement line on an elliptical shape (rotated for 20°)

Case 5: Displaced measurement line on an elliptical shape (rotated for 45°)

Case 6: Displaced measurement line on a triangular shape (oriented along the measurement axis)

Case 7: Displaced measurement line on a triangular shape (rotated for 20°)

Case 8: Displaced measurement line on a triangular shape (rotated for 45°)

Figure 8: Cases of simulating diameter measurement error due to the imperfect measurement direction and geometrical irregularities of the ring gauge.

Results of the simulation are presented in Tables III to VIII. Five different errors d (Cases 2 to 8) and five different angular deviations β (Case 1) were simulated within the boundary values presented in Table II.

Table III: Simulation results for measurement axis displacements on a perfect circle.

Gauge ring diameter ***D*** / mm	**Axis displacement** ***d*** / µm				
	2	**4**	**6**	**10**	**20**
	Error of the measured ring gauge diameter e_d / nm				
10	-1	-3	-7	-20	-80
200	0	0	0	-1	-4

The results in Table III show that the influence of the axis displacement is more critical for small ring diameters. Displacement d = 20 μm is already critical for the targeted measurement uncertainty presented in Table I. Therefore, a displacement d = 10 μm shall not be exceeded.

Table IV: Simulation results for angular adjustment of the measurement axis (caused by a conical shape of the ring – cone axis β).

Gauge ring diameter $\boldsymbol{D}$ / mm	**Axis rotation** $\boldsymbol{\alpha}$ / °				
	0.002	**0.005**	**0.010**	**0.015**	**0.020**
	Error of the measured ring gauge diameter $\boldsymbol{e_d}$ / nm				
10	0.0	0.0	0.2	0.3	0.6
200	0.1	1	3	7	12

The results in Table IV show that the influence of the axis rotation is more critical for big ring diameters. However, the limits of α = 0.02° are not critical for the targeted measurement uncertainty presented in Table I.

Tables V to VII present results for elliptical shape of the ring gage in different orientations to the measurement axis. As it can be quite clearly seen, the orientation of the ellipse has no significant influence on the measurement error. However, the error quite strongly depends on the cylinder shape. The difference between the cylinder diameters (a, b) in the simulation was taken from the actual measurements in the laboratory. The worst case from numerous measurements was evaluated to be $a - b$ = 2 μm.

Table V: Simulation results for measurement axis displacements on a cylindrical shape (the ellipse not rotated – Case 3 in Fig. 8).

Gauge ring diameter $\boldsymbol{D}$ / mm	**Axis displacement** $\boldsymbol{d}$ / μm				
	2	**4**	**6**	**10**	**20**
	Error of the measured ring gauge diameter $\boldsymbol{e_d}$ / nm				
10	1	3	7	20	80
200	0	0	0	1	4

Table VI: Simulation results for measurement axis displacements on a cylindrical shape (the ellipse rotated for 20° – Case 4 in Fig. 8).

Gauge ring diameter $\boldsymbol{D}$ / mm	**Axis displacement** $\boldsymbol{d}$ / μm				
	2	**4**	**6**	**10**	**20**
	Error of the measured ring gauge diameter $\boldsymbol{e_d}$ / nm				
10	1	3	7	20	80
200	0	0	0	1	4

Table VII: Simulation results for measurement axis displacements on a cylindrical shape (the ellipse rotated for 45° – Case 5 in Fig. 8).

Gauge ring diameter $\boldsymbol{D}$ / mm	**Axis displacement** $\boldsymbol{d}$ / μm				
	2	**4**	**6**	**10**	**20**
	Error of the measured ring gauge diameter $\boldsymbol{e_d}$ / nm				
10	1	3	7	20	80
200	0	0	0	1	4

The results in Tables V to VII initiate the same conclusion as those in Table III for ideal circle. Displacement d = 20 μm is already critical for the diameter D = 10 mm for the targeted measurement uncertainty presented in Table II. Therefore, a displacement $d \leq$ 10 μm shall be achieved in the measurement process.

Table VIII: Simulation results for measurement axis displacements on a triangular shape (Reuleaux triangle – Case 6 in Fig. 8).

Gauge ring diameter ***D*** / mm	**Axis displacement** ***d*** / μm				
	2	**4**	**6**	**10**	**20**
	Error of the measured ring gauge diameter e_d / nm				
10	1	3	7	20	80
200	0	0	0	1	4

Analogous to the results for the elliptical shape, the rotation of the shape has no influence on the measurement error. Also in this case it can be concluded that a displacement $d \leq 10$ μm shall be achieved in the measurement process in order not to exceed targeted measurement uncertainty.

5. CONCLUSION

The aim of the presented research work was to develop and validate an original method and procedure for calibrating ring gauges. The method differs significantly from existing methods as the measurement is absolute and we do not need reference rings with metrological traceability at a higher level. The measurement setup used in the research consists of a numerically controlled multi-axis stage, a laser interferometer and a bidirectional inductive 1D probe. We also use this device in the laboratory to calibrate step gauges [10] that are used as the most common measurement standard for checking performance of CMMs [11].

One of the main challenges in the development of the method was the orientation of the ring in the measurement space and the influence of geometric anomalies on the determination of the direction and position of the measurement axis. We decided to solve the problem by simulating different orientations and geometric deviations of the rings from the ideal cylinder. The boundary conditions for the simulations were defined based on the results of previous calibrations in our laboratory and in national European laboratories, which ensure our metrological traceability. A key boundary condition was also the target measurement uncertainty (CMC), which we do not want to exceed with the procedure. Our customers, who in addition to calibration laboratories also include demanding automotive, aircraft and other industries [12-14], are becoming increasingly demanding and require measurement accuracies that are comparable with the accuracies of leading European and global laboratories. The simulations presented have shown that the research hypotheses put forward can be confirmed.

Further research in this area will aim to automate the measurement process and develop a method and procedure for calibrating external diameters with comparable calibration and measurement capability (CMC). In future, we also want to replace the existing He-Ne laser with a diode laser with a wavelength in the IR range in the measurement setup [15-17]. The biggest challenge here is to ensure the metrological traceability of this laser, as no national metrology institute worldwide currently offers the corresponding calibration.

ACKNOWLEDGEMENT

The authors acknowledge the financial support from the Slovenian Research Agency (Research Core Funding No. P2-0190, Grant numbers 1000-20-0552, 6316-3/2018-255, 603-1/2018-16), as well as from the Metrology Institute of the Republic of Slovenia (funding of national standard of length; Contract No. C3212-10-000072). Furthermore, the authors would like to acknowledge the use of research equipment for processing and monitoring the machining and forming processes: Laser measuring systems for machine tools and coordinate measuring machines, procured within the project "Upgrading national research infrastructures – RIUM", which was co-financed by the Republic of Slovenia, the

Ministry of Education, Science and Sport and the European Union from the European Regional Development Fund.

REFERENCES

[1] Carmignato, S.; de Chiffre, L.; Bosse, H.; Leach, R. K.; Balsamo, A.; Estler, W. T. (2020). Dimensional artefacts to achieve metrological traceability in advanced manufacturing, *CIRP Annals*, Vol. 69, No. 2, 693-716, doi:10.1016/j.cirp.2020.05.009

[2] JCGM 200:2012 (2012). *International Vocabulary of Metrology – Basic and General Concepts and Associated Terms (VIM)*, 3rd ed., BIPM-JCGM, Paris, doi:10.59161/JCGM200-2012

[3] Suchanek, P.; Bucki, R.; Postrozny, J. (2023). Modelling and simulation of a decision-making process supporting business system logistics, *International Journal of Simulation Modelling*, Vol. 22, No. 4, 655-666, doi:10.2507/IJSIMM22-4-665

[4] Huang, S.; Chen, J.; Wang, J.; Yao, B.; Li, Y. (2022). Simulation and test of lateral ballast resistance to 1435 mm/1000 mm dual-gauge sleepers, *Technical Gazette*, Vol. 29, No. 1, 215-220, doi:10.17559/TV-20210712053027

[5] Haitjema, H. (2019). Calibration of displacement laser interferometer systems for industrial metrology, *Sensors*, Vol. 19, No. 19, Paper 4100, 21 pages, doi:10.3390/s19194100

[6] Li, Z.; Dai, Y.; Guan, C.; Lai, T.; Sun, Z.; Li, H. (2024). An on-machine measurement technique with sub-micron accuracy on a low-precision grinding machine tool, *Journal of Manufacturing Processes*, Vol. 119, 520-530, doi:10.1016/j.jmapro.2024.03.039

[7] Primozic Merkac, T.; Acko, B. (2010). Comparising measuring methods of pitch diameter of thread gauges and analysis of influences on the measurement results, *Measurement*, Vol. 43, No. 3, 421-425, doi:10.1016/j.measurement.2009.12.012

[8] Tasic, T.; Acko, B. (2011). Integration of a laser interferometer and a CMM into a measurement system for measuring internal dimensions, *Measurement*, Vol. 44, No. 2, 426-433, doi:10.1016/j.measurement.2010.11.002

[9] Klobucar, R.; McCarthy, M.; Acko, B. (2019). Metrological set-up for calibrating 2-dimensional grid plates with sub-micrometre precision, *Measurement*, Vol. 132, 60-67, doi:10.1016/j.measurement.2018.09.035

[10] Šafarič, J.; Klobučar, R.; Ačko, B. (2021). Measurement Setup and Procedure for Precise Step Gauge Calibration, *IEEE Transactions on Instrumentation and Measurement*, Vol. 70, Paper 1009610, 10 pages, doi:10.1109/TIM.2021.3115579

[11] Jotić, G.; Štrbac, B.; Toth, T.; Blanuša, V.; Dovica, M.; Hadžistević, M. (2023). The analysis of metrological characteristics of different coordinate measuring systems, *Technical Gazette*, Vol. 30, No. 1, 32-38, doi:10.17559/TV-20220204091212

[12] Rodriguez, L.; Loyo, J.; Silva, U. (2023). Layout evaluation with the Industry 4.0 approach for a manufacturing laboratory, *International Journal of Simulation Modelling*, Vol. 22, No. 4, 551-561, doi:10.2507/IJSIMM22-4-642

[13] Horvatić Novak, A.; Runje, B.; Samardžić, I.; Maglić, L. (2021). Proposal of a reference object in dimensional measurements using computed tomography, *Technical Gazette*, Vol. 28, No. 5, 1735-1741, doi:10.17559/TV-20200731144524

[14] Pacana, A.; Siwiec, D. (2023). Integrated technique searching causes of quality incompatibilities, *International Journal for Quality Research*, Vol. 17, No. 2, 473-484, doi:10.24874/IJQR17.02-11

[15] Smetana, J.; Di Fronzo, C.; Amorosi, A.; Martynov, D. (2023). Nonlinearities in fringe-counting compact Michelson interferometers, *Sensors*, Vol. 23, No. 17, Paper 7526, 17 pages, doi:10.3390/s23177526

[16] Ghommem, M.; Alattar, B.; Lherbette, M.; Elhady, A.; Abdel-Rahman, E. (2023). Motion measurement methods for nonlinear analysis of electrostatic MEMS resonators, *IEEE EUROCON 2023 – 20th International Conference on Smart Technologies*, 632-637, doi:10.1109/EUROCON56442.2023.10199044

[17] Schödel, R. (Ed.) (2018). *Modern Interferometry for Length Metrology: Exploring Limits and Novel Techniques*, IOP Publishing, Bristol, doi:10.1088/2053-2563/aadddc